

# Dark axisymmetric plasma modes in partially gated two-dimensional electron gas disk

M.V. Cheremisin

*A.F.Ioffe Physical-Technical Institute, St.Petersburg, Russia*

(Dated: May 11, 2023)

The transition from ungated to completely gated disk-shaped two-dimensional gas is studied under extension of the central gate spot. We investigate axisymmetric plasmon excitations spectra which show interchange between neighboring modes caused by abrupt change of carriers screening at the gate boarder. This behavior is totally unexpected within simple scenario of sub-gate gap varying [A.L.Fetter, Phys.Rev.B 33, 5221 (1986)]. Our results provide the accurate identification of axisymmetric plasmon modes recently observed in experiment.

PACS numbers:

Plasma oscillations in two-dimensional(2D) electron gas were first predicted in the 70th by F.Stern[1] for ungated and, then analyzed for gated systems[2]. Over the next decade the plasmon assisted infrared absorbtion[3-6] and emission[7] has been reported. Since Stern's pioneering discovery the enormous efforts were done to clarify the plasmon behavior found to be influenced by magnetic field[8-10], retardation effects[11], sample geometry[12-14] and quality[15-16].

Recently, it has been shown[17-19] that the plasma oscillations for two-dimensional systems with arbitrary attached gates and contacts can be elegantly described in terms of classical theory of electrical circuits with distributed parameters. The proposed LC-approach is extremely powerful for description of plasmon excitations in narrow stripes of 2D gas with periodic grating[20].

In the present paper we will consider two-dimensional electron system of disk geometry shown in Fig.1, inset. The 2D gas mesa of radius  $R$  is grounded peripherally and, moreover, assumed to be embedded into an environment of dielectric constant  $\epsilon$ . The cylindrical slab of the height  $h$  is covered atop by the gate of radius  $r_0$ . For clarity, we further assume a fixed 2D mesa radius  $R$  and, then a variable sizes  $h, r_0$ . We will be interested in study of axisymmetric plasmon modes known to have zero angular momentum[12]. Arguing that axisymmetric plasmon modes are purely radial we makes use of LC-approach[19] in order to find the spectra. Notably the pioneering observation of axisymmetric plasmon was reported recently[21,22].

Within quasistatic approximation the collective plasma excitations in 2DEG can be described by hydrodynamic model[12] which includes Euler and continuity equations. The electric potential of in-plane 2D gas is given by solution of Poisson equation accounting overall the dielectric environment. The set of equations constituent the hydrodynamic model[12] could be linearized with respect to small amplitude of plasma wave excitations. Fortunately, the model could be further simplified[19] down to so-called telegrapher's equations for radial components of in-plane potential  $U$  and the current  $I$ :

$$\frac{\partial U}{\partial r} = -L \frac{\partial I}{\partial t}, \quad (1)$$

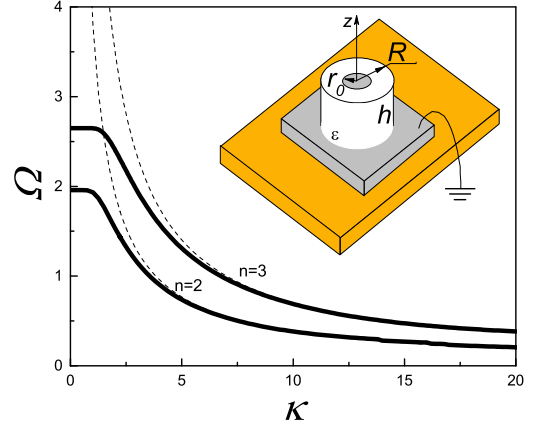


FIG. 1: Inset: the experimental setup. Main panel: the dimensionless frequency  $\Omega = \omega/\omega_0$  vs screening parameter  $\kappa = \sqrt{R/2h}$  for lowest  $m = 2, 3$  plasma modes with  $\alpha_{0m} = 3.831$  and  $7.016$  respectively for totally covered atop 2DEG, i.e. when  $r_0 = R$ . Dashed curves represent the asymptotes  $\Omega = \frac{\alpha_{0m}}{\kappa}$  for highly screened 2D gas.

$$\frac{\partial I}{\partial r} = -C \frac{\partial U}{\partial t}, \quad (2)$$

$$L(r) = \frac{m^*}{e^2 n} \frac{1}{2\pi r}, \quad C(r) = \frac{(1 + \coth(qh))\epsilon q r}{2}. \quad (3)$$

Here,  $L, C$  are the inductance and capacitance per unit length respectively,  $m^*$  and  $n$  are the effective mass and density of 2D carriers. Then,  $q$  is the plasmon wave vector originating from solution of the Poisson equation accounting the actual electrostatic environment.

We now search the solution of Eqs.(1,2) separating the temporal and spatial components for potential  $U = U(r) \exp(i\omega t)$  and current  $I = I(r) \exp(i\omega t)$ . Finally, the equation for radial part of the potential yields:

$$\frac{d^2 U}{d\rho^2} + \frac{1}{\rho} \frac{dU}{d\rho} + U = 0. \quad (4)$$

Here, we introduced the dimensionless radius  $\rho = r/\lambda$ , where  $\lambda = \frac{1}{\omega\sqrt{LC}}$  is the length scale of the problem. The

general solution of Eq.(4) is given by the sum of zero order Bessel functions of first(second) kind, namely

$$U(\rho) = AJ_0(\rho) + BY_0(\rho). \quad (5)$$

The arbitrary constants in Eq.(5) can be found by use of correct boundary conditions.

Let us first consider the simple case of totally gated 2D gas, i.e when  $r_0 = R$  and variable height  $0 < h < \infty$  of the slab. Arguing the potential is finite in the disk center we put  $B = 0$  to avoid divergent behavior of the second term in Eq.(5) at  $\rho \rightarrow 0$ . Noticing that the peripheral current is absent, i.e.  $I(R) \sim \rho \frac{dU}{d\rho} = 0$ , we finally find out the dispersion equation for plasmon excitations

$$\omega\sqrt{LC}R = \alpha_{0m}, \quad (6)$$

where  $\alpha_{0m}$  is the  $m$ th zero of the function  $J_0(x)$ . Using Eq.(3) we re-write Eq.(6) as it follows

$$\omega = v_p \frac{\alpha_{0m}}{R} \cdot \left[ \frac{1 - e^{-2hq}}{2hq} \right]^{1/2}, \quad (7)$$

where  $v_p = \sqrt{\frac{4\pi e^2 nh}{m^* \epsilon}}$  is plasma wave velocity.

For strong screening case  $qh \ll 1$  we obtain the relationship

$$\omega = v_p \frac{\alpha_{0m}}{R}, \quad (8)$$

which is exactly the linear dispersion law[2,12] if one defines wave vector

$$q = \frac{\alpha_{0m}}{R} \quad (9)$$

for present case of axisymmetric plasmon excitations.

In the opposite ungated case  $qh \gg 1$  Eq.(7) provides familiar long-wave dispersion law[1]

$$\omega = \sqrt{\frac{2\pi e^2 n}{m^* \epsilon}} q \quad (10)$$

with the wave vector specified by Eq.(9) as well.

Let's do visualization of the transition from ungated to screened 2D system by fixing the disk radius and, then varying the slab height. It is convenient to introduce the reference value of frequency  $\omega_0 = \sqrt{\frac{2\pi e^2 n}{m^* \epsilon R}}$  and screening parameter  $\kappa = \sqrt{R/2h}$ . Using Eq.(7) we plot in Fig.1 the dimensionless frequency  $\Omega = \omega/\omega_0$  vs  $\kappa$  for lowest axisymmetric modes  $m = 2, 3$ . For highly screening case  $\kappa \gg 1$  one obtains  $\Omega = \frac{\alpha_{0m}}{\kappa}$  being a simple replica of Eq.(8). For ungated 2D gas  $\kappa \ll 1$  we recover the result specified by Eq.(10) as  $\Omega = \sqrt{\alpha_{0m}}$ . The change in axisymmetric mode behavior occurs at  $\kappa \sim 1$  which was not clearly indicated in longstanding classical study[12].

The second part of the present paper concerns more interesting case of partially gated 2D electron system shown in Fig.1, inset. The extension of the central gate

spot would result in a transition from ungated to fully gated 2D gas as well. We now search the spectra of axisymmetric excitations by varying the central gate radius  $0 \leq r_0 \leq R$  and keeping fixed  $h, R$ . Evidence shows that for gated disk(index "1") and ungated hoop(index "2") the in-plane potential can be written as it follows

$$U_1 = A_1 J_0(\rho_1) \quad (11)$$

$$U_2 = A_2 J_0(\rho_2) + B_2 Y_0(\rho_2) \quad (12)$$

$$U_1 = U_2 |_{r=r_0}, U_1' = U_2' |_{r=r_0}, U_2' |_{r=R} = 0, \quad (13)$$

where the dimensionless variable  $\rho_{1,2} = r/\lambda_{1,2}$  are different for gated disk and ungated hoop since  $\lambda_{1,2} = \frac{1}{\omega\sqrt{LC_{1,2}}}$ . Equations(11),(12) have to be solved jointly

with boundary conditions specified by Eq.(13) for continuous potential and current in gated/ungated parts respectively and, then the absence of outgoing current at the slab perimeter. Finally, we obtain cumbersome transcendental dispersion equation

$$J_0(\Omega\kappa\nu)(J_1(\Omega^2\nu)Y_1(\Omega^2) - J_1(\Omega^2)Y_1(\Omega^2\nu)) + \quad (14)$$

$$\frac{k}{\Omega} J_1(\Omega\kappa\nu) [J_1(\Omega^2)Y_0(\Omega^2\nu) - J_0(\Omega^2\nu)Y_1(\Omega^2)] = 0,$$

which can be minimized as it follows

$$D_U \cdot H_I + \frac{k}{\Omega} D_I \cdot H_U = 0. \quad (15)$$

Eq.(15) allows one to obtain the plasmon frequency  $\Omega$  vs dimensionless radii ratio  $\nu = r_0/R$  at certain value of screening parameter  $\kappa$ . Here, we use the notations  $D_I = J_1(\Omega\kappa\nu)$  and  $D_U = J_0(\Omega\kappa\nu)$  for gated disk(D) part. The solutions  $D_{I(U)} = 0$  correspond to zero current at the disk center and, then the zero current(voltage) respectively at the disk circumference. The remaining multipliers, namely  $H_I = J_1(\Omega^2\nu)Y_1(\Omega^2) - J_1(\Omega^2)Y_1(\Omega^2\nu)$  and  $H_U = J_1(\Omega^2)Y_0(\Omega^2\nu) - J_0(\Omega^2\nu)Y_1(\Omega^2)$  correspond to ungated hoop(H) part seen in Fig.1, inset. The transcendental equations  $H_{I(U)} = 0$  define the solution of Bessel Eq.(4) for zero current(voltage) respectively at the internal boarder and, then absence of the current at the outer boarder of the hoop.

For real systems[22] the typical disk size  $R = 0.25\text{mm}$  is much greater than the gate to 2DEG separation is  $h = 370\text{nm}$ , hence we find  $\kappa = 18 \gg 1$ . Assuming that  $\Omega \sim 1$  we conclude that second summand in Eq.(15) prevails. Moreover, the zeroth of transcendental equation  $D_I = 0$  defines, in general, the solution of Eq.(15) in total. The later condition corresponds to axisymmetric plasmon modes excited in a gated part along. It is easy to check that the plasmon modes frequencies are given by asymptotes  $\Omega = \frac{\alpha_{0m}}{\kappa\nu}$  shown by dotted lines in Fig.2. We emphasize that this simple scenario fails when the multipliers from first(second) summand in Eq.(15) vanish simultaneously, i.e. when  $D_U, H_U = 0$ , therefore the dispersion Eq.(15) becomes fulfilled as well. The solutions of equations  $D_U = 0$  and  $H_U = 0$  are shown in

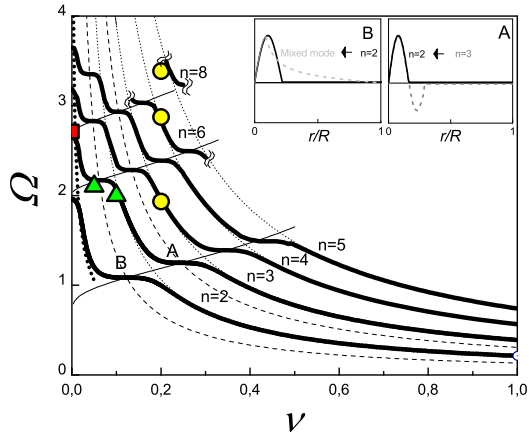


FIG. 2: The dimensionless frequency  $\Omega = \omega/\omega_0$  vs ratio  $\nu = r_0/R$  for lowest  $m = 2.5$  and, partially  $m = 6, 8$  plasma modes plotted for fixed  $\kappa = 18$ . Dotted lines represent the asymptotes  $\Omega = \frac{\alpha_0 m}{\kappa \nu}$  expected for plasmon in the gated part along. Dashed (thin) lines depict  $D_U = 0$  and  $H_U = 0$  solutions respectively. Bold dashed line specifies the "soft" mode asymptote  $\Omega = \frac{1}{\sqrt{\kappa \nu}}$ . Inset A(B): Radial distribution of the current density for intermode transition A(B) shown in the main panel. The experimental data indicated in Table 1 for:  $\square$ -ungated[22] and  $\triangle, \circ$  - partially gated 2D system[21].

Fig.2 by thin and dashed lines respectively. This condition  $D_U, H_U = 0$  is exactly one defines the transition between neighboring axisymmetric modes. To support our reasoning we plot schematically in Fig.2, inset A the spatial distribution of the current for neighboring plasma modes  $m = 2, 3$ . Actually, the transition  $3 \rightarrow 2$  consists of half wavelength shrinking happened at point A in Fig.2.

For small gate sizes when the most place atop the slab is occupied by ungated hoop, the lowest mode  $m = 2$  undergo further transformation. The point of interest B in Fig.2 is still defined by condition  $D_U, H_U = 0$ . However, in the present case the plasmon mode  $m = 2$  is first confined within ultra-narrow gated part and, then is modified entirely by occupation of the ungated part as whole. Let us call further this mode as "soft" mode. In Fig.2 we represent schematically the current spatial distribution for initial  $m = 2$  mode and, finally, the "soft" mode. We

verify the dispersion relation for soft mode follows the asymptote  $\Omega = \frac{1}{\sqrt{\kappa \nu}}$ . In actual fact, the "soft" mode is a precursor of the conventional plasmon in totally ungated 2D system, i.e.  $\Omega = \sqrt{\alpha_0 m}$ .

It is worthwhile to mention with respect to Fig.2 that upon change of the gated part radius  $r_0$  the plasmon frequency follows either  $\omega \sim 1/\sqrt{r_0}$  or  $\omega \sim 1/\sqrt{R}$  dependencies regarding to the actual  $\nu$ -range of interest. Evidently, the latter uncertainty may lead in misunderstanding regarding plasma mode identification.

TABLE I: Axisymmetric plasmon: theory vs experiment

$n$	$h$	$r_0$	$R$	$f_0$	$f_{\text{exp}}$	$\Omega_{\text{exp}}$	Ref.
	( $10^{11} \text{cm}^{-2}$ )	nm	mm	GHz	GHz		
2.6	-	0	0.25	22.1	60.0	2.71	$\square$ [22]
1.0	370	0.05	0.25	13.7	26.5	1.93	$\circ$ [21]
1.0	370	0.05	0.25	13.7	39.4	2.87	$\circ$ [21]
1.0	370	0.05	0.25	13.7	46.4	3.38	$\circ$ [21]
1.0	370	0.05	0.50	9.7	19.4	2.0	$\triangle$ [21]
1.0	370	0.05	1.0	6.9	14.4	2.1	$\triangle$ [21]

Let us compare our results with experimental findings. The data are collected in Table 1 for AlGaAs/GaAs samples[21,22] demonstrated axisymmetric plasmon excitations. Fortunately, a use of dimensionless units allows one to put a different data points on the same plasmon spectra graph in Fig.2. Indeed, for each sample one may calculate the respective reference frequency  $f_0 = \omega_0/2\pi$  and, then find out the ratio  $\Omega_{\text{exp}} = f_{\text{exp}}/f_0$ . The latter can be added into plasmon spectra graph in Fig.2. Note an overall agreement between the experimental data and theory predictions. However, the data shown by circles in Fig.2 demonstrate a puzzling series of high-order plasmon excitations for even numbers  $m = 4, 6, 8$  only.

In conclusion, we investigated the transition from ungated to gated two-dimensional system of disk geometry by means of central spot gate expansion. The discontinuity of gated to ungated part provides the interchange between the neighboring axisymmetric modes. The experimental data for different sample sizes, carrier densities is found to agree well with theory predictions. Our study allows to classify the observed axisymmetric modes.

[1] F. Stern, Phys. Rev. Lett. **18**, 546 (1967).  
[2] A.V. Chaplik, Zh. Eksp. Teor. Fiz. **62**, 746 (1972) [Sov. Phys. JETP **35**, 395 (1972)].  
[3] C.C. Grimes and G. Adams, Phys. Rev. Lett. **36**, 145 (1976).  
[4] S.J. Allen, D.C. Tsui and R.A. Logan, Phys. Rev. Lett. **38**, 98 (1977).  
[5] T.N. Theis, J.P. Kotthaus and P.J. Stiles, Solid State

Comm. **26**, 603 (1978).  
[6] D.Heitmann, J.P. Kotthaus, and E.G. Mohr, Solid State Commun. **44**, 715 (1982).  
[7] D.C. Tsui, E. Gornik, and R.A. Logan, Solid State Comm. **35**, 875 (1980).  
[8] K.W.Chiu and J.J.Quinn, Phys.Rev.B **9**, 4724 (1974).  
[9] M.Nakayama, J.Phys.Soc.Jpn. **36**, 393 (1974).  
[10] V.A. Volkov and S.A. Mikhailov, Sov. Phys. JETP **67**,

- 1639 (1988).
- [11] I.V. Kukushkin, J.H. Smet, S.A. Mikhailov, D.V. Kulakovskii, K.von Klitzing and W. Wegscheider, Phys.Rev.Lett. **90**, 156801 (2003).
- [12] A.L. Fetter, Phys. Rev. B **33**, 5221 (1986).
- [13] Yu.A. Kosevich, A.M. Kosevich, J.C. Granada, Phys. Lett. A, **127**, 52 (1988).
- [14] A.A. Zabolotnykh and V.A. Volkov, JETP Lett **115**, 141 (2022). [ Pis'ma Zh. Eksp. Teor. Fiz. **115**, 163 (2022) ].
- [15] V.I.Falko and D.E.Khmel'nitskii, Zh. Eksp. Teor. Fiz. **95**, 1988 (1989) [Sov. Phys. JETP **68**, 1150 (1989)].
- [16] M.V.Cheremisin, Solid State Comm. **268**, 7 (2017).
- [17] P.J. Burke, I.B. Spielman, and J.P. Eisenstein, Appl. Phys. Lett. **76**, 745 (2000).
- [18] F. Rana, IEEE Trans. Nanotech. **7**, 91 (2008).
- [19] G.C. Dyer, G.R. Aizin, S. Preu, N.Q. Vinh, S.J. Allen, J.L. Reno, and E.A. Shaner, Phys.Rev.Lett. **109**, 126803 (2012).
- [20] G.C. Dyer, G.R. Aizin, S.J. Allen, A.D. Grine, D. Bethke, J. L. Reno, and E.A. Shaner, Nature Photon. **7**, 925 (2013).
- [21] V.M. Muravev, I.V. Andreev, V.N. Belyanin, S.I. Gubarev, and I.V. Kukushkin, Phys. Rev. B **96**, 045421 (2017).
- [22] A.A. Zagitova, V.M. Muravev, P.A. Gusikhin, A.A. Fortunatov, I.V. Kukushkin, JETP Lett. **108**, 446 (2018) [Pis'ma Zh. Eksp. Teor. Fiz. **108**, 478 (2018) ].